Thermoelastic Topology Optimization of Engine Exhaust-Washed Structures with Stress Criteria

Joshua D. Deaton* and Ramana V. Grandhi†
Wright State University, Dayton, OH, 45435

Structures located aft of embedded engines on modern military aircraft, known as engine exhaust-washed structures, are exposed to an extreme thermal loading environment where damaging effects of thermal stresses may lead to premature failure. Since these stresses originate from restrained thermal expansion, design against them involves managing the trade-space between the need for structural stiffening material and the loading generated by that material, which may actually increase stress levels. In this work, thermoelastic topology optimization is utilized in an effort to generate more effect engine exhaust-washed structure designs. It is well known in topology optimization, that in the presence of thermal loading, maximum stiffness objectives generally do not lead to maximum strength structures. Thus, we compare topological results obtained via stiffness-based design criteria to those obtained when including stress criteria in the topology optimization problem including stress-constrained and minimum stress formulations. Different techniques for handling stress constraints in topology optimization are tested for thermal stresses, which is a first in the literature. The final paper will include thermoelastic topology optimization of engine exhaust-washed structure inspired thermoelastic test problems utilizing both stiffness and stress criteria.

Nomenclature

α	=	coefficient of thermal expansion	σ_e	=	elemental stress
β	=	thermal stress coefficient (TSC)	σ_e^r	=	relaxed elemental stress
B	=	Heaviside filter parameter	σ_{PN}	=	p-norm global stress measure
$\boldsymbol{B}_e$	=	strain-displacement matrix for element e	$\bar{\sigma}$	=	allowable stress
c	=	scaling parameter for stress relaxation	P	=	*p-norm* parameter
C	=	compliance	q	=	internal RAMP penalization parameter
$\boldsymbol{C}_e$	=	elasticity matrix for element e	$\boldsymbol{R}$	=	thermal load vector (thermal system)
Δ	=	element center-to-center distance	R	=	RAMP interpolation function
e	=	element number	r_{min}	=	density filter radius
E	=	elastic modulus	T_e	=	temperature of element e
$\boldsymbol{\varepsilon}_e^{th}$	=	thermal strain vector for element e	T_0	=	reference temperature
$\boldsymbol{F}^m$	=	mechanical load vector	$\boldsymbol{T}$	=	nodal temperature vector
$\boldsymbol{F}^{th}$	=	thermal load vector (structural system)	ΔT	=	temperature rise
F	=	reaction force constraint value	$\boldsymbol{U}$	=	nodal displacement vector
$\boldsymbol{F}_e^{th}$	=	thermal load vector for element e	$\boldsymbol{x}$	=	design density variable vector
γ	=	internal parameter for stress relaxation	v_e	=	volume of element e
H_{ei}	=	weight factor for element e to i	x_e	=	design density for element e
l	=	optimization iteration number	$\tilde{x}_e$	=	intermediate density for element e
$\boldsymbol{K}$	=	structural stiffness matrix	$\bar{x}_e$	=	physical density for element e
$\boldsymbol{K_t}$	=	thermal conductivity matrix	x_{min}	=	minimum allowable density
k	=	thermal conductivity			

I. Introduction

Thermal structures have been an active area of research in the aerospace industry since the early 1950s and the advent of supersonic flight. In general the field is concerned with the effects of elevated temperatures or large spatial and temporal temperature gradients on structural components.[1] These effects lead to thermal expansion, that if not properly accounted for, may lead to damaging thermal stresses and component failure. In general, the best practice

*Graduate Research Assistant, Department of Mechanical and Materials Engineering, AIAA Student Member.
†Distinguished Professor, Department of Mechanical and Materials Engineering, AIAA Fellow

to prevent thermal stresses is to allow for thermal expansion. In fact, even allowing a small amount of expansion can significantly reduce or altogether eliminated thermal stresses in most cases.[2] However, in the modern day aerospace industry, increased requirements on mission capability, combat survivability, and versatility of military aircraft necessitate innovative configurations with design scenarios where such a prescription for thermal stresses is not possible. In these situations, platform level design requirements necessitate strict fixivity requirements on critical structural components that are subjected to elevated temperatures.[3]

One of these situations exists in embedded engine aircraft, such as the B-2 Spirit and future concepts, where engines are buried inside the airframe. This configuration allows for a smooth outer mold line (OML), which decreases radar observability in addition to reducing infrared detectability by preventing direct line-of-sight to hot engine components with a ducted exhaust system.[4] The structural components located aft of the embedded engines that make up this exhaust system are known as *engine exhaust-washed structures* (EEWS). A conceptual EEWS configuration is shown in Figure 1.[5]

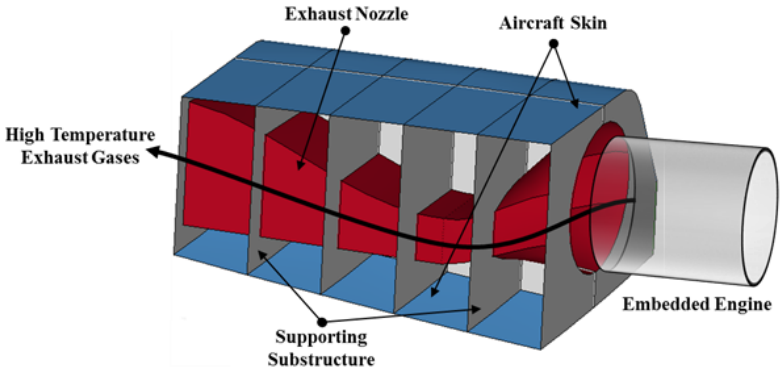

Figure 1. Conceptual engine exhaust-washed structure configuration that would be located aft of embedded engines on a low observable aircraft.

The overall structure consists of an exhaust-washed surface through which high temperature exhaust gases are passed and the supporting substructure that is all contained inside the aircraft skins. In this configuration it is important to note that design constraints placed on the shape of the exhaust nozzle and its fixivity to other components, which result from the desired configuration level performance capabilities, create a situation where it is difficult to freely accommodate thermal expansion of hot structure components. As such, the layout of substructure members to which the exhaust-washed surface is attached is extremely difficult because the loading in the system, which results from restrained thermal expansion and leads to thermal stresses, is directly dependent upon the existence and connectivity of structural material. As a result, improper usage of structural material in a thermal environment in an effort to reduce thermal stresses can actually have the opposite effect in some circumstances, actually *increasing* the stress.[6] This includes the design of primary substructure as shown in Figure 1 and any additional stiffening elements in the system. Since thermal expansion cannot be freely accommodated, an effective structural layout for exhaust-washed structures is one where structural member connectivity allows some expansion where possible, and material is used optimally so as to prevent excessive amounts of loading in the component of interest and adjoining ones.

Topology optimization is a structural design process utilized to determine the connectivity, shape, and location of voids inside a given design domain.[7] Thus, it is a promising tool for managing the challenging trade-spaces related to the structural design of engine exhaust-washed structures, which is fundamentally a material layout problem. When considering the application of topology optimization to the EEWS design problem, one is faced with two primary considerations. The first is related to the multiphysics nature of the domain, where both heat transfer and structural analysis is required to properly model the behavior. The second relates to the consideration of stress criteria, which is a most recent development in topology optimization and one that has yet to be demonstrated with thermal stresses or thermoelastic systems.

While the roots of topology optimization lie in structural design using stiffness or frequency criteria (both of which are purely mechanical responses), the method has been applied to alternative physics problems including heat transfer and thermoelasticity. Early research by Rodrigues and Fernandes, which was based on a homogenization method, presented theory and design cases that later have been used as benchmark problems in many publications.[8] Li et al. utilized evolutionary procedures for thermoelastic topology optimization for both displacement minimization and

for problems with varying temperature fields.[9,10] Sigmund and Torquato used topology design to generate structures with extremal thermal expansion properties and Sigmund utilized multiphysics topology optimization including heat transfer and thermoelasticity in the design of thermal microactuators.[11,12] Jog demonstrated topology optimization for nonlinear thermoelasticity.[13] A primary challenges in thermoelastic topology optimization stems from the use of the common compliance or stiffness objective, which is adopted in most legacy thermoelastic work, in the presence of thermal loading. For density-based methods, these challenges manifest themselves in the form of intermediate density (or "gray" material) in optimal solutions because of the design dependency of thermal loads. Recently, a number of researchers have investigated alternative problem formulations, domain parametrization, and material interpolation schemes to overcome these challenges. Pedersen and Pedersen question the effectiveness of the compliance objective and offer an alternative objective based on uniform energy density for functionally graded structures.[14,15] Gao and Zhang studied the effects of different material interpolation schemes and demonstrate the superiority of the RAMP method over the more popular SIMP method for thermoelastic problems.[16] Xia and Wang applied the level set method, which is an implicit representation of the structure, to circumvent the formation of intermediate material areas.[17] Wang et al. obtain optimal structures with low directional thermal expansion and high stiffness using a bi-objective formulation.[18] Finally, Haney[3] and Deaton and Grandhi[19] utilized alternative problem formulations using fictitious mechanical loading and intuitive constraints to generate desirable thermoelastic performance on EEWS topology design problems.

Despite the fact that stress is a critical consideration in structural design, the majority of development in structural topology design has concentrated on compliance or other global response constraints such as frequency. This is likely due to three primary challenges associated with stresses in topology optimization: (i) the singularity phenomenon, (ii) the local nature of stress, and (iii) the highly non-linear behavior of stress constraints.[20] Early work in the area of stress constrained topology optimization was completed by Duysinx and Bendsøe.[21,22]. More recently, Pereira et al.,[23] Bruggi,[24] Guilherme and Fonseca,[25] Le et al.,[20] París et al.,[26,27] and Lee et al.[28] have studied various aspects of the stress constrained topology optimization problem related to relaxation methods and aggregation techniques for local stress values.

In this work, we seek to directly address the problematic thermal stresses in the design of engine exhaust-washed structures. Since topology optimization with stresses has yet to be demonstrated using thermal loading, we compare multiple methods to accommodate stresses in the optimization problem. Results are also compared against those obtained using stiffness-based formulations for EEWS inspired problems. We also include design-*dependent* heat transfer effects to represent more realistic, spatially varying, temperature loads as demonstrated in Sigmund[12]. This stands in contrast to most examples of thermoelastic topology optimization that are based on design-*independent* thermal loads, which avoids re-analysis of a heat transfer during optimization. Section II of this extended abstract introduces the multiphysics thermoelastic topology optimization formulation including the methods for incorporating stress criteria. Section III introduces the EEWS inspired demonstration problem and preliminary results are discussed in Section IV. Finally, Section V highlights future work that will be included in the final paper.

II. Topology Optimization

In this work, we utilize a finite element (FE) representation of the structure along with the popular density-based method for topology optimization. The design domain is explicitly parametrized using a density function where design variables are taken as the densities of each finite element as $0 < x_{min} \leq x_e \leq 1$. Here, x_{min} is a minimum density parameter used to avoid numerical issues associated with zero density values and x_e is the density design variable for element e.

A. Thermoelastic Finite Element Formulation

A sequential coupling between a steady-state heat transfer problem and the structural system is adopted. The discretized thermoelastic system is modeled by two separate finite element problems for heat transfer and structures, which are both parametrized by the density design variable vector $\mathbf{x}$. These systems are given by Equations 1 and 2, respectively. We simplify the system to assume that all material properties are constant with temperature and we currently study only linear systems for computational efficiency. Nonlinear responses could be considered via an iterative solution procedure and more costly nonlinear sensitivity analysis methods.

$$\boldsymbol{K}_t(\boldsymbol{x}) \cdot \boldsymbol{T}(\boldsymbol{x}) = \boldsymbol{R} \tag{1}$$

$$\boldsymbol{K}(\boldsymbol{x}) \cdot \boldsymbol{U}(\boldsymbol{x}) = \boldsymbol{F}^{m} + \boldsymbol{F}^{th}(\boldsymbol{T}(\boldsymbol{x}), \boldsymbol{x}) \tag{2}$$

In Equation 1, $\boldsymbol{K_t}(\boldsymbol{x})$ is the thermal conductance matrix, $\boldsymbol{T}(\boldsymbol{x})$ is the temperature vector, and $\boldsymbol{R}$ is the thermal load vector. In Equation 2, $\boldsymbol{K}(\boldsymbol{x})$ is the structural stiffness matrix, $\boldsymbol{U}(\boldsymbol{x})$ is the displacement matrix, $\boldsymbol{F}^{m}$ is the design-independent mechanical load vector, and $\boldsymbol{F}^{th}(\boldsymbol{T}(\boldsymbol{x}), \boldsymbol{x})$ is the design-dependent vector of loads that results from thermal expansion of the structure due to the temperature response obtained as a solution of Equation 1.

System matrices $\boldsymbol{K}(\boldsymbol{x})$ and $\boldsymbol{K}_t(\boldsymbol{x})$ are assembled in the usual way as sums over element matrices. They are parametrized similar to the work of Sigmund using methods consistent with typical density-based topology optimization[12]; however a non-SIMP interpolation scheme discussed in the following section is used. The design-dependent thermal load, $\boldsymbol{F}^{th}$, in the structural system is parametrized by using the thermal stress coefficient (TSC) introduced by Gao and Zhang.[16] The nodal load vector for the element e may be written as:

$$\boldsymbol{F}_e^{th} = \int_{\Omega_e} \boldsymbol{B}_e^T \boldsymbol{C}_e \boldsymbol{\varepsilon}_e^{th} d\Omega \tag{3}$$

By definition, $\boldsymbol{B}_e$ is the element strain-displacement matrix, which consists of derivatives of the element shape functions that are independent of topology design variables. $\boldsymbol{C}_e$ is the element elasticity matrix, which for isotropic materials can be written as the linear function of elastic modulus:

$$\boldsymbol{C}_e = E(x_e) \cdot \bar{\boldsymbol{C}}_e \tag{4}$$

where $\bar{\boldsymbol{C}}_e$ consists of constant terms related to the material constitutive relationship and $E(x_e)$ is determined via a material interpolation scheme using the elemental density variable x_e. $\boldsymbol{\varepsilon}_e^{th}$ is the thermal strain vector for the element given by:

$$\boldsymbol{\varepsilon}_e^{th} = \alpha(x_e)(T_e - T_0)\boldsymbol{\phi}^T \tag{5}$$

Here, $\alpha(x_e)$ is the thermal expansion coefficient, T_e is the elemental temperature determined from thermal analysis, T_0 is the reference temperature, and ϕ is [1 1 1 0 0 0] for three-dimensions and [1 1 0] for two-dimensions. Substitution of Equations 4 and 5 into Equation 3 yields:

$$\boldsymbol{F}_e^{th} = E(x_e)\alpha(x_e)(T_e - T_0) \int_{\Omega_e} \boldsymbol{B}_e^T \bar{\boldsymbol{C}}_e \boldsymbol{\phi}^T d\Omega \tag{6}$$

We note that both $\alpha(x_e)$ and $E(x_e)$ are dependent upon topological design variables and thus both necessitate material interpolation. With popular penalty methods, the question of how aggressively to penalize each quantity relative to each other arises. Note that the choice of the penalty on elastic modulus also affects the stiffness matrix. To simplify this, the thermal stress coefficient (TSC) is introduced, which is the product of the elastic modulus and coefficient of thermal expansion:

$$\beta(x_e) = E(x_e)\alpha(x_e) \tag{7}$$

The TSC is then treated as an inherent material property with its own interpolation. Thus, $\boldsymbol{F}_i^{th}$ can be rewritten as:

$$\boldsymbol{F}_e^{th} = \beta(x_e) \cdot (T_e - T_0) \int_{\Omega_e} \boldsymbol{B}_e^T \bar{\boldsymbol{C}}_e \boldsymbol{\phi}^T d\Omega \tag{8}$$

where $\beta(x_e)$ varies with x_e to accommodate the design dependency of thermal loading and the remainder of the relationship is constant with respect to topology variables in the optimization.

After first solving Equation 1 to determine the temperature response and subsequently solving Equation (2) to obtain nodal displacements, element stresses are determined as a post processing step:

$$\boldsymbol{\sigma}_e = \boldsymbol{C}_e \boldsymbol{B}_e \boldsymbol{U}_e - \boldsymbol{C}_e \boldsymbol{\varepsilon}_e^{th} \tag{9}$$

In addition, to allow for the comparison to stiffness based design objectives, the compliance C in the thermoelastic system may be determined as:

$$C = (\boldsymbol{F}^{m} + \boldsymbol{F}^{th})^T \boldsymbol{U} = \boldsymbol{U}^T \boldsymbol{K} \boldsymbol{U} \tag{10}$$

B. Interpolation Scheme and Filtering

The selection of the interpolation scheme in topology optimization in the presence of design dependent loading is extremely important, especially for stiffness design problems. While the most popular interpolation scheme is undoubtedly the Solid Isotropic Material with Penalization (SIMP) method, it has been shown to induce undesirable parasitic effects in optimal solutions for these types of problems.[16] This primarily occurs because the SIMP model becomes insensitive at densities near zero and the volume constraint is generally not active when using compliance or stiffness objectives. An alternative interpolation introduced by Stolpe and Svanberg, called the Rational Approximation of Material Properties (RAMP),[29] has demonstrated superior performance in thermal problems. While these issues have not been documented in the literature when including stress criteria in the optimization problem, we adopt the RAMP interpolation model to allow for the additional study of stiffness-based problem formulations for comparison. The penalization function for RAMP is given as:

$$R(x_e) = \frac{x_e}{1 + q(1 - x_e)} \tag{11}$$

where q is an internal parameter analogous to the penalization exponent in SIMP. The parametrization for thermal conductivity k, elastic modulus E, and thermal stress coefficient β are given by Equations 12 to 14 where subscript zero denotes a baseline value and each physical quantity has its own penalization parameter q.

$$k(x_e) = \frac{x_e}{1 + q_k(1 - x_e)} k_0 \tag{12}$$

$$E(x_e) = \frac{x_e}{1 + q_E(1 - x_e)} E_0 \tag{13}$$

$$\beta(x_e) = \frac{x_e}{1 + q_\beta(1 - x_e)} \beta_0 \tag{14}$$

In order to prevent checker-boarding, enforce length scale, and to further force black/white solutions, a recent Heaviside projection filter is utilized.[30] This projection filter is an extension of the basic density filter given by:

$$\tilde{x}_e = \frac{1}{\sum_{i \in N_e} H_{ei}} \sum_{i \in N_e} H_{ei} x_i \tag{15}$$

where $\tilde{x}_e$ is an intermediate density value, N_e is the set of elements i for which the center-to-center distance $\Delta(e, i)$ to element e is smaller than the filter radius r_{min} and H_{ei} is a weight factor given by:

$$H_{ei} = max\,(0, r_{min} - \Delta(e, i)) \tag{16}$$

Intermediate densities obtained from Equation 15 are projected into the physical domain using a smoothed Heaviside step function:

$$\bar{x}_e = 1 - e^{-B\tilde{x}_e} + \tilde{x}_e e^{-B} \tag{17}$$

Here, $\bar{x}_i$ is called the physical density and the parameter B controls the smoothness of the approximation. For B equal to zero, Equation 17 gives the value of the original density filter and B approaching infinity, Equation 17 approaches a true step function. In order to avoid local optima and ensure differentiability in the optimization, a continuation scheme is used where B is gradually increased. We note that after the application of filters, the design variable densities and the physical densities actually representing the structure differ. Since physical densities are utilized to determine system responses, the chain rules in Equations 18 and 19 and the derivative of the Heaviside function in Equation 20 must be included in sensitivity analysis for any system response f:

$$\frac{\partial f}{\partial x_j} = \sum_{e \in N_j} \frac{\partial f}{\partial \tilde{x}_e} \frac{\partial \tilde{x}_e}{\partial x_j} = \sum_{e \in N_j} \frac{1}{\sum_{i \in N_e} H_{ei}} H_{je} \frac{\partial f}{\partial \tilde{x}_e} \tag{18}$$

$$\frac{\partial f}{\partial \tilde{x}_e} = \frac{\partial f}{\partial \bar{x}_e} \frac{\partial \bar{x}_e}{\partial \tilde{x}_e} \tag{19}$$

$$\frac{\partial \bar{x}_e}{\partial \tilde{x}_e} = \beta e^{-B\tilde{x}_e} + e^{-B} \tag{20}$$

C. Stress-based Design Criteria

The following sections highlight the treatment of stress criteria in the topology optimization formulation. This treatment is consistent with the methods utilized by Le et al. for purely mechanical load cases.[20] To the authors' knowledge, this work represents the first treatment of stress-constraints for thermoelastic topology optimization.

1. Stress Relaxation

The relaxation of stresses in topology optimization is necessary to circumvent the so called "singularity" problem, which manifests itself when optimal topologies belong to degenerate subspaces of the feasible design space. These occur when one or more design variables equals zero in the global optimal solution. Unfortunately, convergence to these singular topologies is practically impossible with gradient based optimizers unless the degenerate subspaces are eliminated via relaxation. In this work, relaxation is performed by applying material interpolation to stress values to penalize stresses in a manner similar to other quantities:

$$\sigma_e^r(x_e) = x_e^{1/2}\sigma_e \tag{21}$$

Here, σ_e is the solid stress obtained from finite element analysis and $\sigma_e^r(x_e)$ is the relaxed stress quantity. We note that with this relaxation when $x_e = 0$, the relaxed stress is zero, which corresponds to zero stress in void regions. When $x_e = 1$, the relaxed stress is equal to the solid stress. The relaxed stress is then used to define the stress measure, von Mises stress for example, that is in turn used to define design metrics.

2. Normalized Global Stress Measure

In the ideal case of topology optimization with stress constraints, one stress constraint per element is enforced to ensure that the maximum stress remains below an acceptable level. This implies that both the number of design variables and the number of constraints is equal to the number of elements, which is inherently large for typical topology optimization problems. Thus, sensitivity analysis by either the direct or adjoint method is equal and prohibitively costly. To reduce this burden a single aggregated global stress constraint may be used. Since a simple maximum stress constraint is not differentiable, one may use the *p-norm* or the *Kreisselmeier-Steinhauser (KS)* function, both of which attempt to approximate the maximum stress using a continuous function. In this work we utilize the normalized global stress measure developed by Le et al.[20]. The measure is based on the general *p-norm* measure given by:

$$\sigma_{PN} = \left(\sum_{e=1}^{N} v_e \sigma_e^P\right)^{1/P} \leq \bar{\sigma}_{PN} \tag{22}$$

where P is the stress norm parameter, v_e is the element e solid volume, and $\bar{\sigma}_{PN}$ is an allowable *p-norm* stress. It is assumed a single stress criterion is imposed and the stress is non-negative. Since in reality, the p-norm stress measure lacks physical meaning (as opposed to the maximum stress in the structure), a normalization procedure is employed. The *normalized* global stress measure uses information from the previous optimization iteration to scale the global *p-norm* measure such that it better approximates the actual maximum stress in the structure. The maximum stress σ_{max}^{I-1} and *p-norm* value σ_{PN}^{I-1} from the previous optimization iteration $I-1$ are utilized to define the evolving normalized global measure at each iteration I as:

$$\sigma_{max} \approx c\sigma_{PN} \leq \bar{\sigma} \tag{23}$$

Here, $\bar{\sigma}$ is a physically based allowable stress value and c is calculated at each optimization iteration $I \geq 1$ as follows:

$$c^I = \gamma^I \frac{\sigma_{max}^{I-1}}{\sigma_{PN}^{I-1}} + (1-\gamma^I)c^{I-1} \tag{24}$$

The above parameter $\gamma^I \in (0, 1]$ controls the variations of c between successive optimization iterations $I-1$ and I. $0 < \gamma^I < 1$ is chosen if c tends to oscillate between iterations, otherwise $\gamma^I = 1$ is used. $\gamma^1 = 1$ always for the first iteration. As topology optimization converges, the variations between displacement and stress responses decreases such that eventually Equation 23 holds true and the *p-norm* constraint value closely approximates the maximum stress. We note that this yields a non-differentiable constraint because the value of c is changed in a discontinuous manner.

According to the literature, this does not create convergence issues because in later iterations, the changes become smaller and reduce the effects of non-differentiability and inconsistency.[20]

III. Demonstration Cases

The design optimization problems solved in this work are motivated by the deformation and stress response of engine exhaust-washed structures. Figure 2 shows the characteristic deformation of the conceptual EEWS introduced earlier. We note from the figure the primary response is the large out-of-plane deformations of the hot exhaust-washed nozzle surface. This out-of-plane deformation generates thermal stresses in the unsupported structural panels primarily in regions where they join to substructure members. This is highlighted in Figure 3, where we see areas of high stress along the edges of an exhaust-washed structural panel. Due to the design dependency of thermal loading, these stresses are extremely challenging to manage. In fact, conventional room temperature design techniques may actually lead to an increase in stress, which has been demonstrated with only a simple thickness increase of the panel.[6] An effective method for stress reduction is one that optimally places material in the appropriate locations to reduce stresses without increasing thermal loading. Ideally, thermal expansion internal to the structure is also allowed. Thus, we attempt to apply topology optimization to accomplish these basic design objectives.

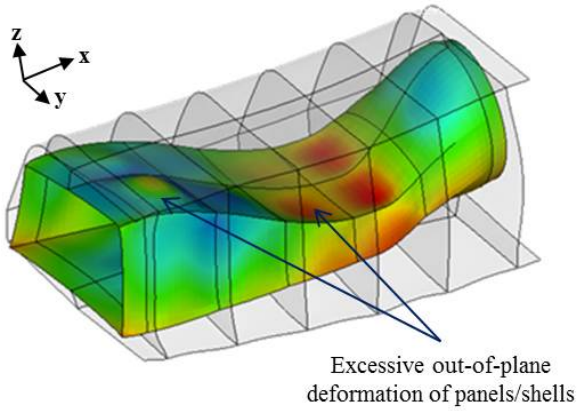

Figure 2. Response of a conceptual EEWS system exhibiting out-of-plane deformation of exhaust-washed structural panels.

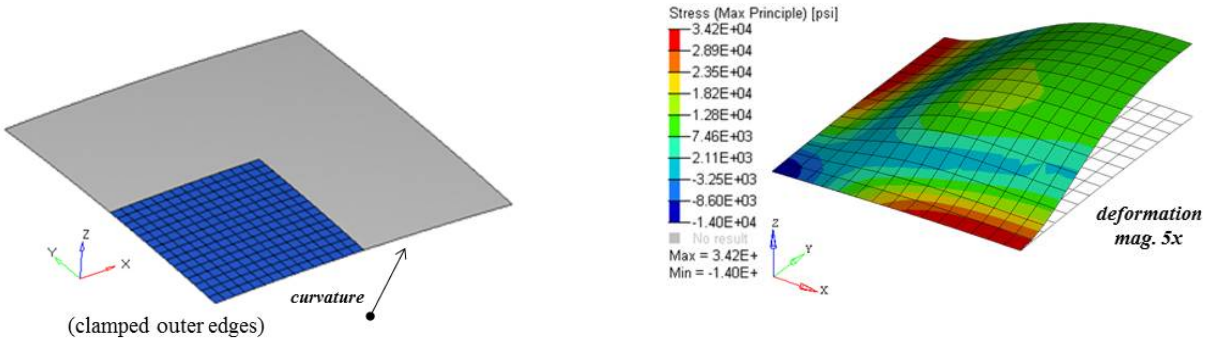

Figure 3. (a) Characteristic panel with quarter symmetry finite element model and (b) its stress response. Note areas of high thermal stress along edges.

We simplify this basic response of out-of-plane deformation leading to excessive thermal stresses by reducing the scenario to a simple 2D geometry for preliminary investigations of topology optimization. As shown in Figure 4, a portion of the exhaust nozzle surface (originally represented as a curved shell) is now idealized as a semi-infinite curved strip. The edges of the strip are clamped, which represents the worst case scenario for adjoining to surrounding

substructure. When subjected to an elevated temperature, the strip will deform out of plane and areas of high stress will result near clamped boundaries in a manner identical to the 3D curved shell and full EEWS model. To apply topology optimization, we assume that a designable region exists below the original thin shell geometry in which a stiffening structure or substructure may be generated. This new design domain is shown in Figure 5. Structural

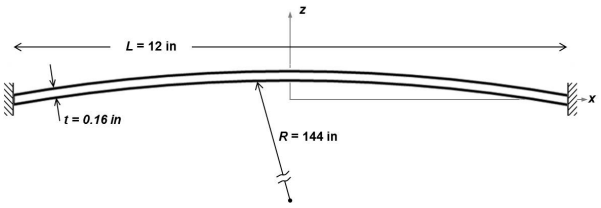

Figure 4. Simplified representation of EEWS panel as semi-infinite curved strip.

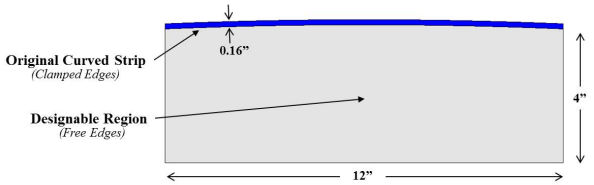

Figure 5. Topological design domain (gray) in relation to the original curved strip geometry, which is taken as a non-designable region (blue).

boundary conditions consist of fully clamped conditions at the edges of the original thin shell geometry (non-design domain). Any edge that forms inside the designable region during the topology optimization remains as a traction free boundary. Two different thermal loading cases are considered. The first case consists of simply a uniform temperature rise ΔT across the entire domain. The second case is meant to more realistically capture the actual loading scenario of an EEWS system. It consists of a convection boundary condition from a high temperature source into the top of the non-design domain. This represents heating by high temperature exhaust gases over the exhaust-washed surface in an EEWS system. Design dependent convection boundaries are also applied to the designable region to represent cooling, which is accomplished in an EEWS by venting to ambient air. The design dependent convection boundaries are handled in topology optimization using the method developed by Bruns.[31] These thermal load cases are shown in Figure 6.

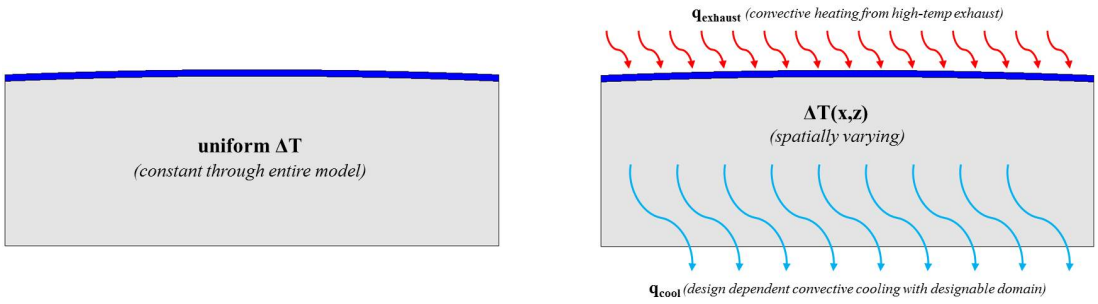

Figure 6. Case I: Design-independent thermal load case with uniform temperature rise. Case II: Design-dependent thermal loading with convective boundary conditions of EEWS structure.

The designable domain is discretized using bilinear quadrilateral finite elements with 152 elements in the horizontal direction and 50 elements in the vertical direction. This results in a design problem with 7600 topology design variables. Note that due to the curvature of the top of the design space, the elements are not perfectly rectangular. Material properties are taken as those of high temperature titanium (Ti-6Al-2Sn-4Zr-2Mo) and are assumed independent of temperature at this time.

Three formulations of topology optimization problems, based both on stress and stiffness criteria are now summarized. Sensitivities of the implicitly defined quantities in the following problem statements are determined via the adjoint method. The MMA algorithm is used to solve the resulting constrained optimization problems. For the stress-constrained problem we minimize volume subject to a stress constraint computed using the normalized global stress relation introduced previously. The optimization problem is stated:

Minimize: Volume: $V = \sum_{e=1}^{N} v_e x_e$
Subject to: Stress: $c\sigma_{PN} \leq \bar{\sigma}$

In the stress minimization problem, we minimize the *p-norm* stress computed via Equation 22 and place a constraint on the amount of structural material that may be used via a volume fraction constraint:

Minimize: Stress: σ_{PN}
Subject to: Volume: $V = \sum_{e=1}^{N} v_e x_e \leq V_f$

For additional comparison, we also introduce a stiffness-based design formulation originally developed by Deaton and Grandhi.[19] This method utilizes a fictitious mechanical load, whose direction is chosen based on a set of application criteria, in addition to constraints on volume fraction and the reaction force at the boundaries of the model. With proper choice of fictitious load and reaction force constraint, a topology is generated with a compliance-based problem that has amenable thermoelastic performance. From a thermal stress perspective, this method is effective because it generates a structure with stiffness aligned to prevent out-of-plane deformation, which we recall is the primary source of stresses in EEWS systems. One drawback is that since no stress constraints are explicitly defined, the excessive stresses in the substructure that develops in the designable region may still exist. The basic optimization problem for this stiffness-based design formulation is given as:

Minimize: Compliance: $C = \boldsymbol{U}^T \boldsymbol{K}\boldsymbol{U}$ where U satisfies $\boldsymbol{K}\boldsymbol{U} = \boldsymbol{F}^f$
Subject to: Volume: $V = \sum_{e=1}^{N} v_e x_e \leq V_f$
Reaction Force: $F \leq F_L$where F is determined from $\boldsymbol{K}\boldsymbol{U} = \boldsymbol{F}^{th}$

IV. Preliminary Results

In this section we highlight some preliminary results for the stiffness-based design case of uniform thermal loading. The final paper will include results of stress-based design cases for both design-independent and design-dependent thermal loading cases in addition to stiffness-based results for design-dependent loads. Designs obtained via topology optimization using the stiffness-based technique for two different volume fractions are given in Figure 7.

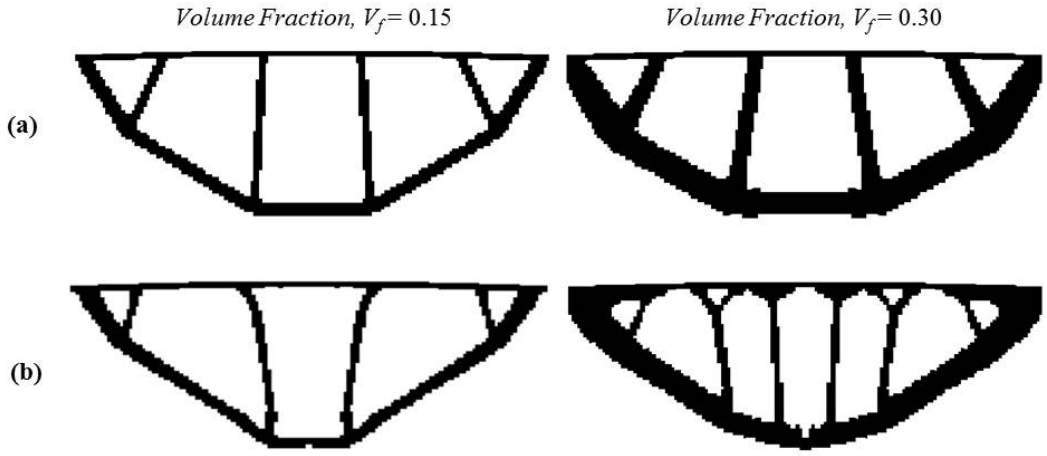

Figure 7. Topology optimization results for two volume fractions using different stiffness-based problem formulations.

In the figure, the results shown in (a) were obtained using a formulation that lacked a reaction force constraint, while (b) includes a reaction force constraint that must be less than 2.5 times the reaction force of the unstiffened beam strip configuration. In both cases topologies are generated that exhibit multiply connected domains with the majority of structural stiffness to prevent out-of-plane deformation of the original beam strip geometry. This is evident in the deformation response of the 0.15 volume fraction designs shown in Figure 8 (note deformation is magnified 5 times in the figure). We see that whereas the original unstiffened strip (or 3D panel) deformed upwards out-of-plane, the new

stiffened design is actually pulled downwards by the stiffening material. This occurs due to the the thermal expansion of the stiffening structure. Such behavior and a suitable design is likely only obtained via topology optimization. Since excessive thermal stresses resulted from out-of-plane deformation, reducing this deformation also reduces these stresses.

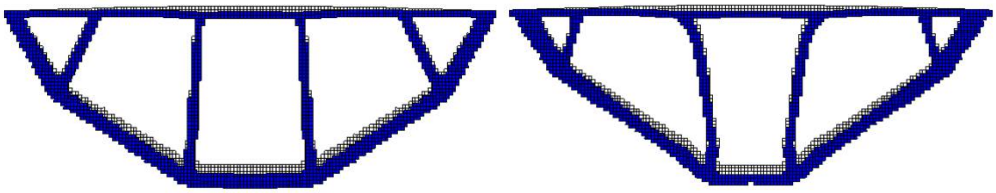

Figure 8. Undeformed configuration (white) and deformed configuration (blue) of topological results obtained via stiffness-based formulation (deformation magnified x5).

It is anticipated that a minimum volume stress-constrained result will be similar, but have the advantage of accounting for stress levels in the newly generated substructure. In the previous results, considerations for reduced stress are only made for the original strip geometry. Reducing In the larger design scenario, a likely failure due to thermal stresses may have simply been moved to another location. More directly accounting for stresses throughout is the proper design solution. We also anticipate that a minimum stress volume-constrained formulation will generate a structure with more uniform stress profile throughout.

V. Future Work

The final version of the paper and conference presentation will include a comprehensive comparison of topology optimization results for stiffness and stress-based design criteria. This includes the cases for both design-dependent and design-independent thermal loads as discussed previously. The concept of regionalized stress measures will also be explored to improve local control of stress levels as highlighted by Le et al.[20] Discussion of the numerical behavior of the stress measures in the topology optimization will also be given to benchmark their contribution to obtaining black/white designs. It is anticipated that by including stress constraints in the design problem, or purely attempting to minimize stress in the structure, some of the issues that are evident with traditional compliance minimization and thermal loads may be avoided.

It is of merit to note that the results of the final paper will include the first documented application of stress criteria to thermoelastic topology optimization problems. This is important because to date, the bulk of thermoelastic topology publications have utilized simply a compliance objective, which not only has been documented to create numerical issues, but also has been questioned as a valid design objective. This is extremely evident in problems like the exhaust-washed structures explored here, where a minimum compliance structure is likely non-optimal from a stress point-of-view, which is of paramount concern in nearly all thermal structures designs.

References

[1]Thornton, E.A., *Thermal Structures for Aerospace Applications*, AIAA Education Series, AIAA, Reston VA, 1996.

[2]Gatewood, B.E., *Thermal Stresses*, McGraw-Hill Book Company, Inc., New York, NY, 1957.

[3]Haney, M.A., "Topology Optimization of Engine Exhaust-Washed Structures," Ph.D. Dissertation, Department of Mechanical and Materials Engineering, Wright State University, Dayton, OH, 2005.

[4]Paterson, J., "Overview of Low Observable Technology and Its Effects on Combat Aircraft Survivability," *Journal of Aircraft*, Vol. 36, No. 2, 1999, pp. 380-388.

[5]Deaton, J.D. and Grandhi, R.V., "Thermal-Structural Design and Optimization of Engine Exhaust-Washed Structures," AIAA-2011-1903, 52nd AIAA/ASME/ASCE/AHS/ASC Structures, Structural Dynamics and Materials Conference, Denver, CO, April 2011.

[6]Haney, M.A. and Grandhi, R.V., "Consequences of Material Addition for a Beam Strip in a Thermal Environment," *AIAA Journal*, Vol. 47, No. 4, 2009, pp. 1026-1034.

[7]Bendsøe, M.P. and Sigmund, O., *Topology Optimization: Theory, methods and Applications*, 2nd ed., Springer-Verlag, Berlin, Germany, 2003.

[8]Rodrigues H. and Fernandes, H., "A material based model for topology optimization of thermoelastic structures," *International Journal for Numerical Methods in Engineering*, Vol. 38, 1995, pp. 1951-1965.

[9]Li Q., Steven G.P., and Xie Y.M., "Displacement minimization of thermoelastic structures by evolutionary thickness designs," *Computer Methods in Applied Mechanics and Engineering*, Vol. 179, 1999, pp. 361-378.

[10]Li. Q., Steven, G.P., and Xie, Y.M., "Thermoelastic topology optimization for problems with varying temperature fields," *Journal of Thermal Stresses*, Vol. 24, 2001, pp. 347-366.

[11]Sigmund, O. and Torquato, S., "Design of materials with extreme thermal expansion using a three-phase topology optimization method," *Journal of the Mechanics and Physics of Solids*, Vol. 45, 1997, pp. 1037-1067.

[12]Sigmund, O., "Design of multiphysics actuators using topology optimization - Part I: One-material structures," *Computer Methods in Applied Mechanics and Engineering*, Vol. 190, 2001, pp. 6577-6604.

[13]Jog, C, "Distributed-parameter optimization and topology design for non-linear thermoelasticity," *Computer Methods in Applied Mechanics and Engineering*, Vol. 132, Nos. 1-2, 1996, pp. 117-134.

[14]Pedersen, P. and Pedersen, N.L., "Strength optimized designs of thermelastic structures," *Structural and Multidisciplinary Optimization*, Vol. 42, 2010, pp. 681-691.

[15]Pedersen, P. and Pedersen, N.L., "Interpolation/penalization applied for strength design of 3D thermoelastic structures," *Structural and Multidisciplinary Optimization*, Vol. 45, 2012, pp. 773-786.

[16]Gao, T. and Zhang, W., "Topology optimization involving thermo-elastic stress loads," *Structural and Multidisciplinary Optimization*, Vol. 42, 2010, pp. 725-738.

[17]Xia, Q. and Wang, M.,Y., "Topology optimization of thermoelastic structures using level set method," *Computational Mechanics*, Vol. 42., No. 6, 2008, pp. 837-857.

[18]Wang, B., Yan, J., and Cheng, G., "Optimal structure design with low thermal directional expansion and high stiffness," *Engineering Optimization*, Vol. 43, No. 6, 2011, pp. 581-595.

[19]Deaton, J.D. and Grandhi, R.V., "Stiffening of Restrained Thermal Structures via Topology Optimization," *Structural and Multidisciplinary Optimization*, submitted August 2012.

[20]Le, C., Norato, J., Bruns, T., Ha, C., and Tortorelli, D., "Stress-based topology optimization for continua," *Structural and Multidisciplinary Optimization*, Vol. 41, 2010, pp. 605-620.

[21]Duysinx, P. and Bendsøe, M.P., "Topology optimization fo continuum structures with local stress constraints," *International Journal for Numerical Methods in Engineering*, Vol. 43, No. 2, 1998, pp. 1453-1478.

[22]Duysinx, P. and Bendsøe, M.P., "New devleopment in handling stress constraints in optimal material distribution," *In: Proc. 7th AIAA/USAF/NASA/ISSMO Symposium on Multidisciplinary Analysis and Optimization. A collection of technical papers (held in St. Louis, Missouri)*, Vol. 3, 1998, pp. 1501-1509.

[23]Pereira, J.T., Fancello, E.A., and Barcellos, C.S., "Topology optimization of continuum structures with material failure constraints," *Structural and Multidisciplinary Optimization*, Vol. 26, 2004, pp. 50-66.

[24]Bruggi, M., "On an alternative approach to stress constraints relaxation in topology optimization," *Structural and Multidisciplinary Optimization*, Vol. 36, 2008, pp. 125-141.

[25]Guilherme, C.E.M. and Fonseca, J.S.O., "Topology optimization of continuum structures with ε-relaxed stress constraints," In: Alves, M. and da Costa Mattos, H.S. (eds), *Solid Mechanics in Brazil*, Vol. 1, 2007, pp. 239-250.

[26]París, J., Navarrina, F., Colominas, I., and Casteleiro, M., "Block aggregation of stress constraints in topology optimization of structures," *Advances in Engineering Software*, Vol. 41, 2010, pp. 433-441.

[27]París, J., Navarrina, F., Colominas, I., and Casteleiro, M., "Improvements in the treatment of stress constraints in structural topology optimization problems," *Journal of Computational and Applied Mathematics*, Vol. 234, 2010, pp. 2231-2238.

[28]Lee, E., James, K.A., Martins, J.R.R.A., "Stress-constrained topology optimization with design-dependent loading," *Structural and Multidisciplinary Optimization*, doi 10.1007/s00158-012-0780-x, 2012.

[29]Stolpe, M. and Svanberg, K., "An alternative interpolation scheme for minimum compliance topology optimization," *Structural and Multidisciplinary Optimization*, Vol. 22, 2001, pp. 116-124.

[30]Guest, J.K., Prévost, J.H., and Belytschko, T., "Achieving minimum length scale in topology optimization using nodal design variables and projection functions," *International Journal for Numerical Methods in Engineering*, Vol 61, 2004, pp. 238-254.

[31]Bruns, T.E., "Topology optimization of convection dominated, steady-state heat transfer problems," *International Journal for Heat and Mass Transfer*, Vol. 50, 2007, pp. 2859-2873.